IOP Conference Series: Earth and Environmental Science

PAPER • **OPEN ACCESS**

Interannual variability of Indonesian throughflow in the Flores Sea

To cite this article: P Y Putriani *et al* 2019 *IOP Conf. Ser.: Earth Environ. Sci.* **278** 012064

View the article online for updates and enhancements.

This content was downloaded from IP address 120.234.63.196 on 08/11/2019 at 13:23

Interannual variability of Indonesian throughflow in the Flores Sea

P Y Putriani[1*], A S Atmadipoera[1] and D Nugroho[2]

[1]Department Marine Science and Technology, Faculty of Fisheries and Marine Science, Bogor Agricultural University, Bogor, Indonesia
[2]Agency for Marine and Fisheries Research and Human Resources, Ministry of Marine Affairs and Fisheries, Jakarta, Indonesia

*E-mail: yulinaaputt@gmail.com

Abstract. The main branch of Indonesian Throughflow (ITF) from Makassar Strait passes through Flores Sea. The variance of ITF transport volume was influenced by climate phenomenon such as El Nino Southern Oscillation (ENSO). This research was conducted to describe the relationship between the ENSO and the ITF transport variability. This relationship was explored using data from INDESO model 2008- 2015. The variability of transport volume was analyzied using continous wavelet transform and band-pass analysis. Water circulation was analyzed by summing up the average of water current and sea temperatures. The Flores ITF was a portion of Makassar ITF and Eastern ITF that enter via Lifamatola Passage. The flow in the upper layer was intensified during the west monsoon while in the thermocline layer was intensified during the east monsoon. Flores ITF moved along the northern part of Flores Island and was dominated by zonal velocity component.

Keywords: ENSO, Flores Sea, Indonesian throughflow, sea temperatures, water current

1. Introduction

A portion of water mass from Pacific Ocean that moves to Indian Ocean through Indonesia archipelago is well known as Indonesian Throughflow (ITF) [1, 3]. This water mass crossing the archipelago through Makassar Strait, Maluku Sea, and Halmahera Sea and exits through Lombok Strait, Ombai Strait, and Timor Sea [4]. About 20% of the ITF that passes Makassar Strait exits Lombok Strait while the rest moves from Banda Sea and exit via Ombai Strait and Timor Sea [5]. Lombok's ITF branch off, a part of it exited trough Lombok Strait and the rest flowing to southern part of Flores Sea [6]. The volume of the ITF transport fluctuates under the influence of ocean-atmosphere interaction. Asian-Australian monsoon, El Nino/La Nina Southern Oscillation (ENSO), and Indian Ocean Dipole are three of factors that affect ITF transport volume.

The ENSO was identified where warm pool at the center of Pacific Ocean shifts and follows atmospheric phenomenon. During El Nino, the sea level is lower in Pacific Ocean with a consequence in weakened ITF transport [7, 8]. The upper layer is highly affected by monsoon while the middle-bottom layer is affected by ITF [9]. So far, the variability on the ITF volume transport in Flores Sea and its relation to the ENSO have not been studied. This paper provides some findings on the circulation of ITF in the upper layer and

Content from this work may be used under the terms of the Creative Commons Attribution 3.0 licence. Any further distribution of this work must maintain attribution to the author(s) and the title of the work, journal citation and DOI.
Published under licence by IOP Publishing Ltd

bottom layer of Flores Sea, *i.e.* estimate of the ITF transport volume, its variability and the relation of ITF and ENSO.

2. Materials and Methods

2.1. Data

This study utilized data from INDESO model which was limited for an area between 5.6-9.178°S and 118-124.5°E (Flores Sea) (figure 1) and for a period of January 1st 2008 to December 31st 2015.

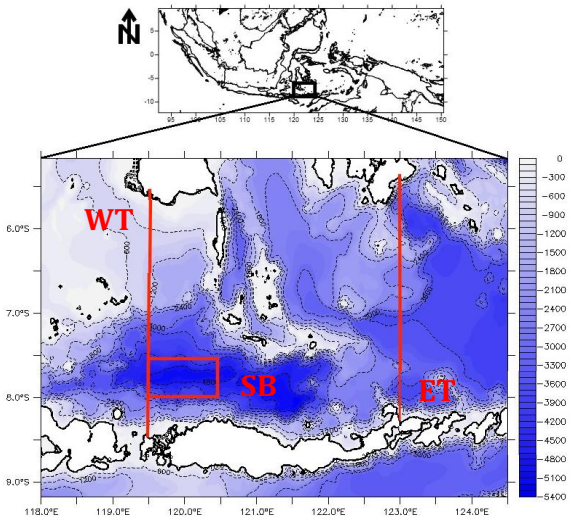


Figure 1. Research location indicating position of western transects (WT) and eastern transects (ET), sampling box (SB).

Estimates of sea current, sea surface temperature (SST) and sea level from INDESO model were validated by data from satellite observation, *i.e.* Global Ocean Data Assimilation Experiment (GODAE) High Resolution SST Pilot Project (GHRSST-PP) for SST, and Jason-3, Sentinel-3A, HY-2A, Saral/AltiKa, Cryosat-2, Jason-2, Jason-1, T/P, ENVISAT/ GFO, and ERS1/2 satellite observation for sea level. Steps in processing SST and SSH data from satellite observations.

2.2. Data Analysis

Data from INDESO model were processed aas described in the flow chart in figure 2.

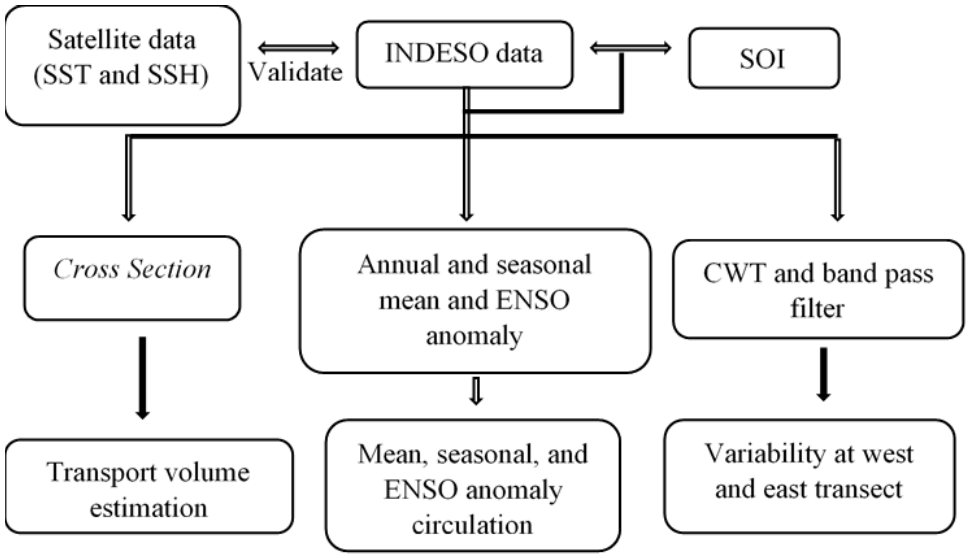


Figure 2. Data processing flow chart.

Southern Oscillation Index (SOI) was used as an indicator for determining El Nino and La Nina phenomenon (figure 3). This index using sea surface pressure difference between Tahiti (Eastern Pacific Ocean) and Darwin Nnorthern Australia). SOI above +7 indicating La Nina occurrence while SOI below -7 indicating El Nino. The values of the index used in this research were obtained from www.bom.gov.aucimate/ which can be written as:

$$SOI = 10\frac{A_{tek}}{SD_A} \quad (1)$$

Data from June 2010 – May 2011 for strong La Nina, November 2008 – March 2009 for weak La Nina, and November 2014 – December 2015 for strong El Nino. While the situation during 2013 was used as normal year, the values of SOI during the study periode are shown in figure 3.

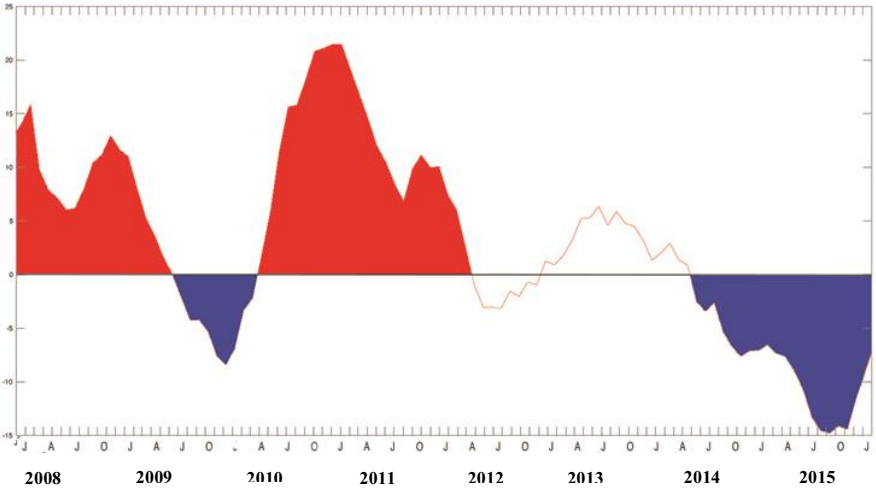


Figure 3. SOI time series from 2008 until 2015. Indicating La Nina (red), El Nino (blue) and normal year (white).

Correlational statistics and root mean square error were used to validate the estimates of sea current, sea surface temperature (SST) and sea level generated by the INDESO model. Correlational statistics can be writen as (2) [10] as for RSME written as (3) [11]:

$$R = \frac{C}{SxSy} \tag{2}$$

Root mean square error (RSME) was calculated from model data root mean square or can be written as:

$$RSME = \sqrt{\frac{1}{n}\sum_{i=1}^{n} e_i^2} \tag{3}$$

SST and water circulation at certain time were acquired from sea temperature and current means. SST data were overlaid with current vector and visualized using Ferret. Sea temperature and current means ($\bar{x}$) can be written as [11]:

$$\bar{x} = \frac{1}{N}\sum_{i=1}^{N} xi \tag{4}$$

Current anomaly during ENSO phenomenon, sea current at certain time was subtracted by mean current or can be written as:

$$Current\ anomaly = Ti - \bar{T} \tag{5}$$

Transport volume (Mx) was estimated using integral of current zonal component (u) from –D depth to surface along transect build in studied area following a formula from [12]:

$$Mx \equiv \int \int_{-D}^{0} u\, dx\, dz \tag{6}$$

Transport variability was calculated using continuous wavelet transform (CWT) on each transect. This analysis understanding non-stationer signal which amplitude and frequency change depending on time. CWT used “major wavelet” which was translated on certain time (τ) and dilated on certain amplitude (a) [13]:

$$\psi_{\mathrm{b,a}}(t) = \frac{1}{a}\psi\left(\frac{t-b}{a}\right) \tag{7}$$

$$\psi(t) = \pi^{1/4} e^{-t^2/2} e^{i\omega_0 t}$$

Inter-annual signal on transport volume variability was identified using band-pass analysis. The results were used to determine the relationships between the ENSO and the variability of ITF transport.

3. Result and Discussion

3.1. Data validation

The estimates of sea surface temperature (SST) and sea level from both INDESO model and observed by satellites from 2008 until 2015 are presented in figure 4.

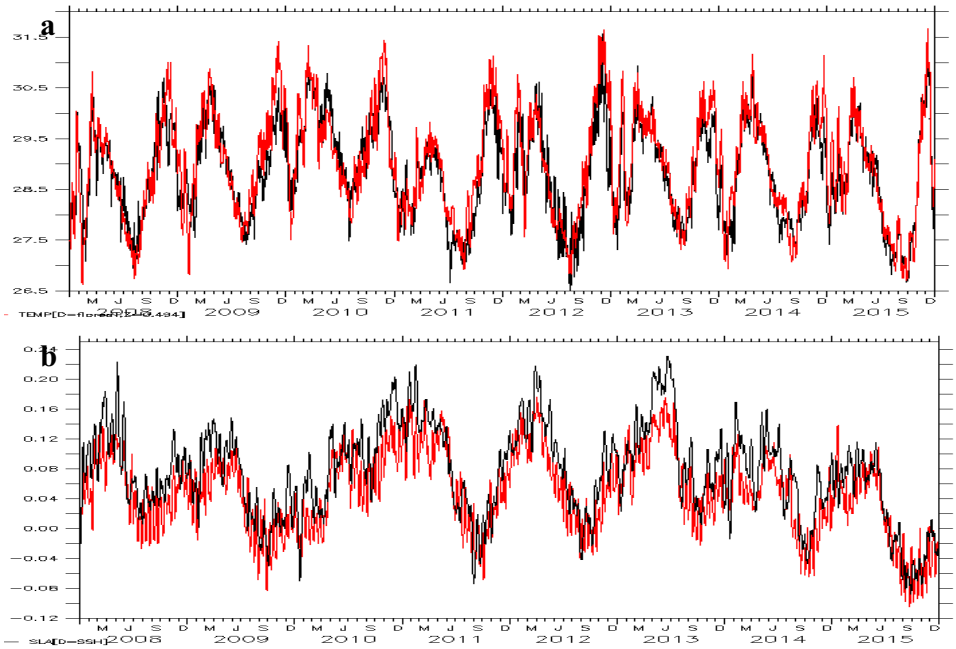


Figure 4. Sea surface temperature (a) and sea level (b) for INDESO model estimates (red) and satellite observation (black) from 2008 until 2015 in the studied area.

The correlational coefficient between SST estimates from INDESO model and satellite-observed data was 0.898. Such coefficient indicates a strong relationship between them. The annual fluctuation of SST shows a semi-annual pattern. The SST was at the warmest during the slowest wind surface which occurred during a period of monsoonal transition (April and November). During the peaks of both west and east monsoons the wind surface speed reached its highest that caused high mixing in the upper layer waters [14].

The correlational coefficient between SSH estimates from INDESO model and satellite-observed data was 0.852. SSH was at the lowest during the 2nd seasonal transitional period (Sep - Oct - Nov) and at the highest during the 1st seasonal transition period (Mar - Apr - May) through the east monsoon (Jun - Jul - Aug). The RSMEs for the SST data was 0.48 and for the SSH was 0.58. These Based on these correlational values and RSMEs, it can be concluded that the INDESO-generated estimates sufficiently represented field condition.

3.2. Water circulation and temperature in the upper and thermocline layers.

The water circulation in the upper and thermocline layers can be determined from the mean current velocity and sea temperature from 2008 until 2015. Overlay of mean current vector and sea temperature is shown on figure 5.

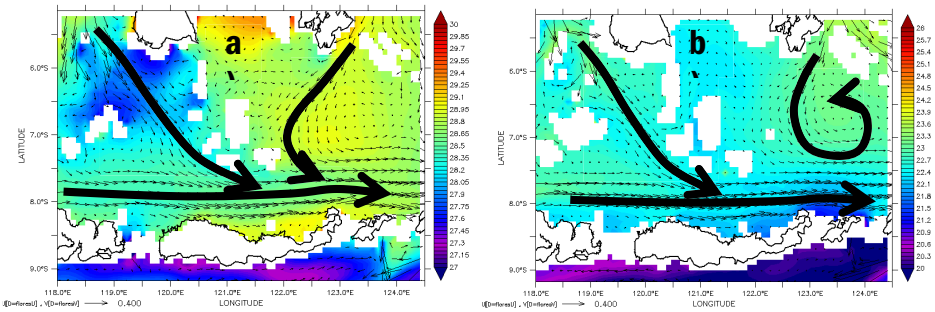


Figure 5. Circulation and sea temperature on upper layer (a) and thermocline layer (b).

The Flores ITF was originated from Makassar ITF and the Eastern ITF enters from Lifamatola Passage [2]. The Makassar ITF branched off to Flores Sea and to Lombok Strait and recirculated to Bali Sea and entering Flores Sea [6].

Current speed in the upper layer ranging between 0.2 m/s to 0.4 m/s; its peak was at Flores Sea. The water temperature from Makassar Strait is cooler (27-28 ^{o}C) than the Eastern ITF (28-29 ^{o}C). Water temperature from Makassar Strait was consistently cooler when entering Flores Sea and Banda Sea [15]. [2] identified this warmer water (29-30 ^{o}C) at 125^{o} E and 5^{o} S. These two water met at the southern part of Flores Sea and formed mixed water with temperature around 28 ^{o}C (Ilahude and Gordon 1996). In the thermocline layer, the Eastern ITF was recirculated due to Ekman force. The current speed in this layer ranged from 0.2 m/s to 0.4 m/s. The sea temperature distributed evenly with a range of 22 ^{o}C to 23 ^{o}C.

3.3. Annual upper and thermocline circulation.

Annual water circulation was acquired from monthly means of sea temperature and water current from 2008 - 2015. This circulation and temperature represented intra-seasonal event in the study area. The water circulations during the west monsoon and east monsoon in the upper layer and thermocline layer were described in figure 6.

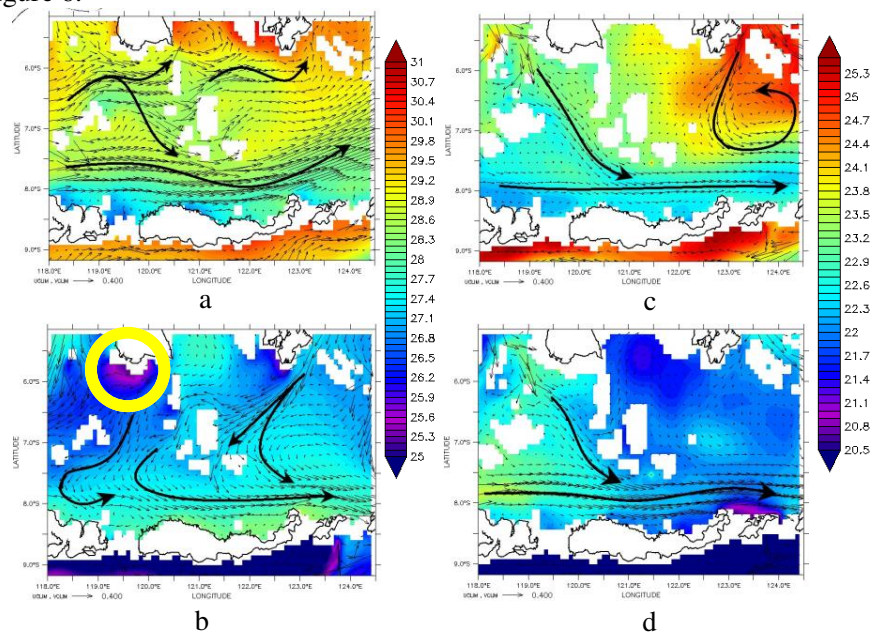


Figure 6. Annual water circulation on upper and thermocline layer when west monsoon and east monsoon. (upper layer (a) west monsoon; (b) east monsoon; thermocline layer (c) west monsoon; (d) east monsoon).

In the upper layer, the sea temperature ranged from 25 °C to 31 °C. The sea temperature during west monsoon to transitional season ranged from 27°C to 30°C while during the east monsoon was 26-29°C. The circulation was affected mainly by surface wind [2, 16]. During the west monsoon, the Eastern ITF disappeared and pushed away by water from Java Sea [16]. The Eastern ITF appeared again during the east monsoon while upwelling occurred around the southern Makassar indicated by colder water (yellow circle).

In the thermocline layer, the water temperature ranged from 21°C to 25°C. Both Makassar Strait ITF and Eastern ITF constantly appeared each month but the later became weaker during the east monsoon. Though it disappeared in upper layer, the Eastern ITF in the thermocline layer clearly existed.

3.4. Cross section and anomaly circulation on ENSO year

Water circulation and sea temperature anomaly during La Nina (2010-2011), El Nino (2014-2015), and normal year (2013) are described in figure 7. The sea temperature anomaly during La Nina period was positive (0.2-0.9°C) which means the sea temperature was warmer than the normal year. In contrast, the sea temperature anomaly was negative (-1.5°C to -0.2°C) indicating the water is colder than the normal year. During El Nino, the depth of thermocline layer was shallower causing the upper layer colder [17]. The water current speed during the El Nino was weaken, but during La Nina it was not significantly different to its normal year.

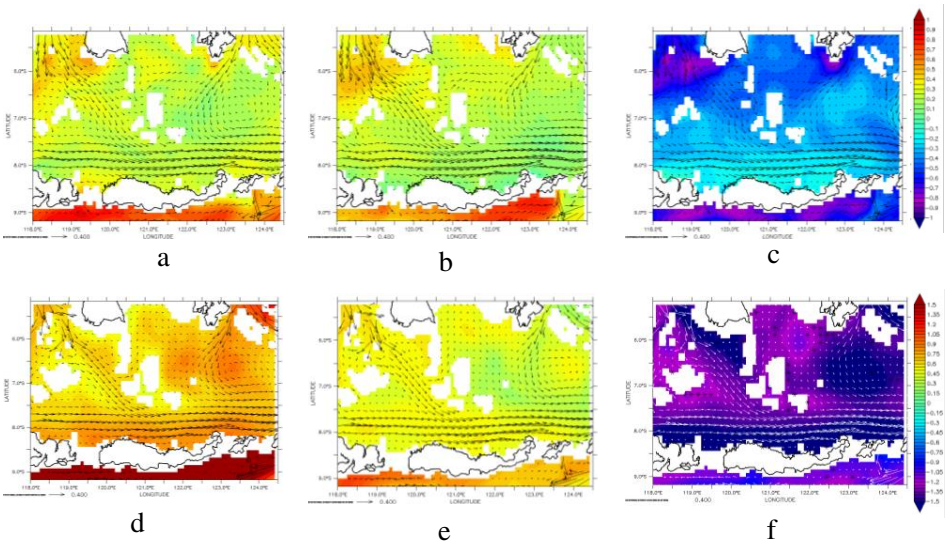


Figure 7. Water circulation and sea temperature anomaly on upper layer and thermocline layer during La Nina, El Nino, and normal year. (Upper layer: (a) La Nina 2010-2011; (b) Normal 2013; (c) El Nino 2014-2015; thermocline layer: (d) La Nina 2010-2011; (e) Normal 2013; (f) El Nino 2014-2015).

Flores ITF (black circle) represented in figure 8. On west transect current on eastern part of transect is input from Makassar Strait. While on east transect eastern part, there is current moving to west that is input from Lifamatola Passage. On both transect Flores ITF persistently moving on southern part of Flores Sea [18].

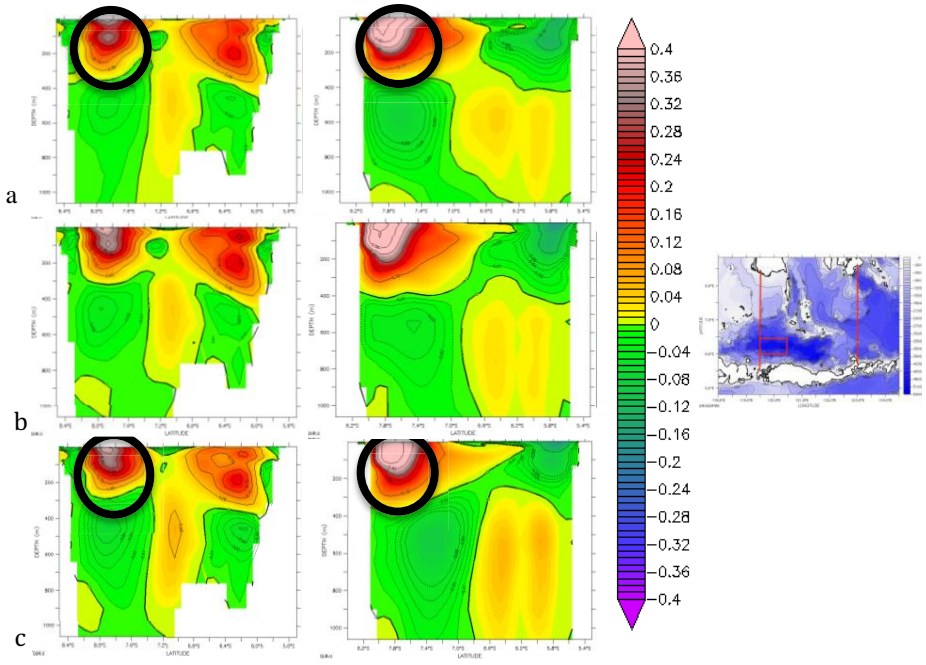


Figure 8. Current zonal component cross section during La Nina (2010-2011) (a), normal year (2013) (b) and El Nino (2014-2015) (c).

During La Nina period, the water current speed was intensified and the water mass transport was deeper, a contrast to El Nino period when water current was weaker and the transport depth was shallower (closer to the sea surface). The transport volume during normal year was 6.7 Sv (WT) and 8.3 Sv (ET), while on El Nino decreased to 5.2 Sv (WT) and 5.6 Sv (ET). During strong la Nina (2010-2011) the transport volume was lower than normal year, i.e. 5.9 Sv (WT) and 7.3 Sv (ET) respectively. Larger transport volume occurred during weak La Nina (2008-2009).

During La Nina (2008-2009), the sea temperature anomaly was much higher than normal year. The current was much intensified both on upper layer and thermocline layer (figure 9). The transport depth was much deeper too. Transport volume on this period was 7.3 Sv (WT) and 9 Sv (ET). The la Nina (2008-2009) coincided with west monsoon.

3.5. Transport variability and its relation to ENSO

The total water mass transport in the upper layer (0-50 m) and thermocline layer (50-1000 m) with SOI are described in figure 10. The upper layer water mass transport fluctuated annual with peaks in July-August, with influence of surface wind. As [2, 5, 16] stated that the water circulation in the upper layer was mainly affected by surface wind. While the water mass transport in thermocline layer fluctuated according to the SSH fluctuation. The sea level difference between the Pacific Ocean and the India Ocean was the biggest during the east monsoon causing larger volume transport during this season [19].

The temporal pattern in water mass transport during the thermocline layer was similar to the SOI pattern, indicating the inter-annual signal have strong influence on the water mass transport in the thermocline layer. The transport variability from wavelet analysis is presented in figure 11 showing intra-seasonal (20-90 days), semi-annual (180 days), and annual (360 days). The inter-annual fluctuation shown from band-pass analysis represented on figure 12 indicating the inter-annual signal of water mass transport is stronger in thermocline layer.

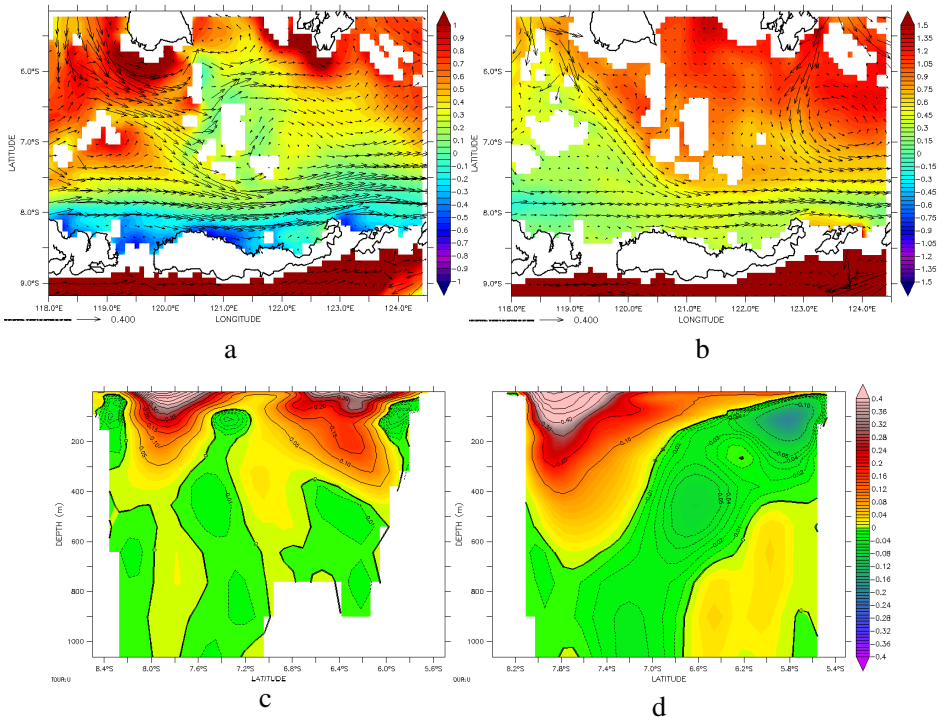


Figure 9. Circulation and sea temperature on upper layer and thermocline layer and current zonal component cross section during La Nina (2008-2009). (a. Upper layer 16 m depth; b. thermocline layer 110 m; c. transport volume 5.9 Sv (WT); d. Transport volume 7.3 Sv (ET)).

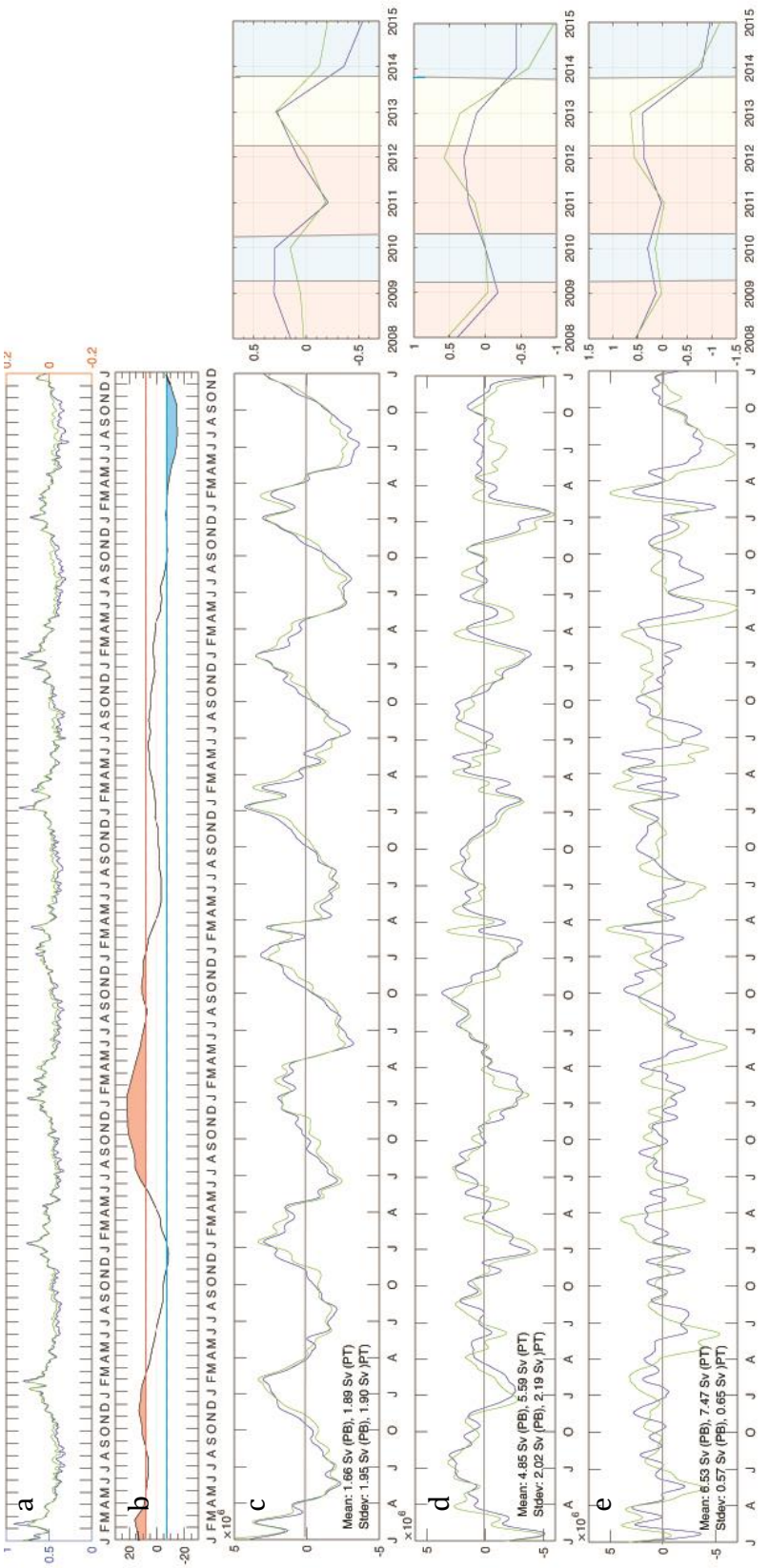


Figure 10. Surface wind speed (a), Flores ITF on upper layer (c) and thermocline layer (d) and total transport (e) (west transect (blue) and east transect (green)) compared to SOI (b). Diagram on right side is mean transport from each year.

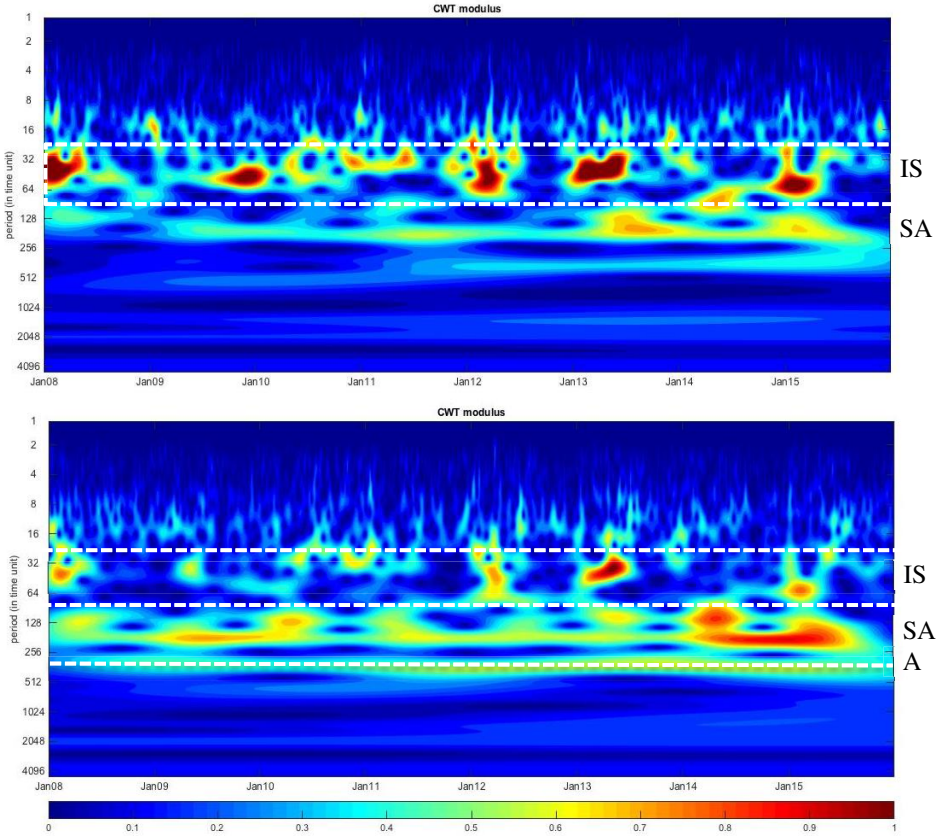


Figure 11. Wavelet analysis to determine volume of water mass transport variability in the western transect (WT, a) and eastern transect (ET, b) show Intra-Seasonal (IS), Semi-Annual (SA) and Annual (A) variability.

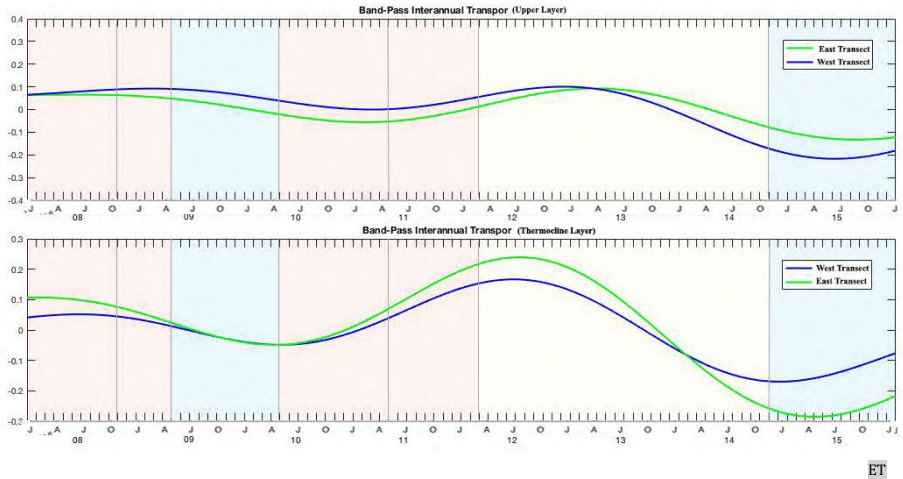


Figure 12. Inter-annual signal for water mass transport in upper layer and thermocline layer. Blue line represent western transect and green line represent eastern transects.

4. Conclusion

The Flores ITF was originated from two areas, *i.e.* Makassar Strait and Lifamatola Passage. Water circulation in the upper layer was mainly affected by surface wind while in the thermocline layer was affected by sea level difference. The Flores ITF main axis persistently moved along the southern part of Flores Sea and dominated by zonal component. The water mass transport depth was deeper during la Nina even and its water mass transport was higher. The wavelet analysis indicated intra-seasonal, semi-annual, and annual variabilities. The inter-annual signal is shown from band-pass analysis.

References

[1] Wyrtki K 1961 Pyhsical oceanography of the Southeast Asian Water *Naga Report. **2***
[2] Gordon A L, Ffield A and Ilahude A G 1994 Thermocline of the Flores and Banda Seas *J. Geophys. Res.* **99** 18235-18242
[3] Atmadipoera A S, Molcard R, Madec G, Wijffels S, Sprintall J, Koch-Larrouy A, Jaya I and Supangat A 2009 Characteristics and variability of the Indonesian throughflow water at the outflow straits *J. Deep-sea Res. I.* **56** 1942-2954
[4] Fieux M, Molcard R and Ilahude A G 1996 Geostrophic transport of the Pacific-Indian Ocean throughflow. *J. Geophys. Res.* **101** 12421-12432
[5] Sprintall J 2009 Indonesian Throughflow *Encyclopedia of Ocean Sciences*. **2** 237-243
[6] Atmadipoera A S dan Hassanah P 2017 Karakter dan variabilitas Arlindo Flores dan koherensinya dengan Arus Pantai Selatan Jawa *JITKT*. **9**(2) 537-556
[7] Safitri M, Cahyarini S Y and Putri M R 2012 Variasi arus Arlindo dan parameter oseanografi di Laut Timor sebagai indikasi kejadian ENSO *JITKT*. **4**(2) 369-377
[8] Susanto R D, Field A, Gordon A L and Adi T R 2012 Variability of Indonesian throughflow within Makassar Strait, 2004-2009 *J. Geophys. Res.***117** 1-16
[9] Sprintall J dan Liu T 2005 Ekman mass and heat transport in the Indonesian seas *Oceanography* **50**(4) 88-97
[10] Emery W J dan Thomson R E 2014 *Data Analysis methods in Physical Oceanography* (Waltham: Elsevier)
[11] Chai T dan Draxier R R 2014 Root mean square error (RMSE) or mean absolute error (MAE)? Arguments against avoiding RMSE in the literature *Geosci. Model. Dev*. **7** 1247-1250
[12] Stewart R H 2002 *Introduction to Physucal Oceanography* (Calvestone: Dept. of Oceanography Texas A&M University)
[13] Risien C M, Reason C J C, Shillington F A dan Chelton D B 2004 Variability in satellite winds over the Benguela upwelling system during 1999-2000 *J. Geophys Res.* **109**
[14] Nababan B, Rosyadi N, Manurung D, Natih N M and Hakim R 2016 The seasonal variability of sea temperature and chlorophyll-a concentration in the south of Makassar Strait *Procedia Environ. Sci.* **33** 583-599
[15] Ilahude A G and Gordon A L 1996 Thermocline stratification within the Indonesian seas *J. Geophys Res.* **101** 12401-12409
[16] Du Y and Qu T 2010 Three inflow pathways of the Indonesian throughflow as seen from the simpel ocean data assimilation *J. Dyn. Atmos.Ocean.* **50** 233-256
[17] Bray N A, Hautala S, Chong J and Pariwono J 1996 Large-scale sea level, thermocline, and wind variations in the Indonesian throughflow region *J. Geophys. Res.* **101**(C5): 12239-12254
[18] Syamsudin F, van Aken H M, Kaneko A 2010 Annual variation of the southern boundary current in the Banda Sea. *J. Dyn. Atmos. Oceans.* **50** 129-139.

[19] Wyrtki K 1987 Indonesian throughflow and the associated pressure gradient *J. Geophys. Res.* **92**(C12): 12941-12946